The radiation-grafting of vinylbenzyl chloride onto poly(hexafluoropropylene-co-tetrafluoroethylene) films with subsequent conversion to alkaline anion-exchange membranes: Optimisation of the experimental conditions and characterisation.

Henryk Herman, Robert C. T. Slade* and John R. Varcoe

Chemistry, The University of Surrey, Guildford GU2 7XH, United Kingdom.

Tel: +44 (0)1483 686855 Fax: +44 (0)1483 686851

*Author for correspondence: E-mail: r.slade@surrey.ac.uk

Poly(hexafluoropropylene-co-tetrafluoroethylene) (FEP) was successfully radiation-grafted with vinylbenzyl chloride (VBC). Subsequently amination with trimethylamine followed by ion exchange with aqueous hydroxide yielded alkaline anion-exchange membranes (AAEMs). Experimental parameters were established for maximising the degree of grafting (d.o.g.); the optimum treatment duration for maximum amination was also established. The graft penetration at different degrees of grafting was investigated and related to the grafting conditions. The stabilities of the grafted membranes and the final AAEMs were thoroughly investigated using thermogravimetry (TG/DTA). The ion-exchange capacities (IECs), water uptake levels, and thicknesses of the AAEMs were measured. These AAEMs have potential for application in low temperature fuel cell systems.

Keywords: Radiation-Grafting, Alkaline Anion-Exchange Membrane, Fuel Cell

1. Introduction

There has been considerable recent interest on clean air technologies for power generation for both stationary and mobile applications. A significant proportion of this has concentrated on fuel cell technology [1], which has been known since the early nineteenth century but where the technology has matured into genuine applicability only recently. For mobile applications, the emphasis has been placed on lower temperature types (< 150°C) including hydrogen fuelled (overall reaction: $H_2 + O_2 \rightarrow H_2O$) alkaline fuel cells (AFCs) and proton-exchange membrane fuel cells (PEMFCs), and the direct methanol fuel cell (DMFC) analogue of the latter (overall reaction: $CH_3OH + 3/2O_2 \rightarrow CO_2 + 2H_2O$) [2]. DMFCs are of primary interest in the field of mobile devices (*e.g.* laptop computers) due to ease and speed (instantaneous) of refuelling and the large energy densities of the methanol fuel [3].

There is extensive worldwide research being conducted on replacement proton exchange membranes (PEMs) [4] and electrocatalysts for DMFCs [5]. The main problems with current generation PEMs (such as Nafion® produced by DuPont) are high methanol permeabilities (from anode to cathode), which result in wasted fuel and low power densities [6] and cost. The electrooxidation of methanol ($6e^-$ reaction) is inherently sluggish, which reduces performances further and leads to the requirement for complex and expensive catalysts (*e.g.* Pt/Ru). The interest in AFCs stems from the high power densities achievable with cheap and simple non-noble metal catalysts [7]. However, AFCs have not been amenable to operation with methanol, as oxidation of methanol produces CO_2, which poisons the liquid alkaline electrolytes (normally KOH(aq)) by the formation of carbonate and hydrogen carbonate.

This study concerns the development of novel membranes for potential application in both methanol and hydrogen fuelled cells, with direct applicability to low temperature DMFCs for portable devices. Strategic methodology involves a hybrid approach combining the advantages (and complimentary behaviours) of DMFCs, PEMFCs and AFCs. This approach involves solid-state *alkaline-form anion-exchange membranes* (AAEMs). The use of AAEMs in DMFCs will allow reduction of the effects of methanol permeabilities in a number of ways. The conduction pathway of the OH^- ions proceeds from the cathode to the anode (opposite to that of current fuel cells involving PEMs) and opposes the direction of methanol flux through the membrane leading to an intrinsic reduction in methanol transport. Electrocatalysis in alkaline media also allows the use of a wider range of catalysts, including cheaper non-noble metals. This larger repertoire of catalysts should allow the selection of a cathode catalyst that does not oxidise methanol, unlike current generation platinum cathode catalysts, which will result in reduced overpotentials arising from methanol crossover. Cheaper and simpler methanol oxidation catalysts would also be feasible for the anode.

A significant proportion of previous fuel cell membrane research has examined the radiation-grafting of styrene onto polyethylene films, partially fluorinated films such as poly(vinylidene fluoride) (PVDF) and poly(ethylene-co-tetrafluoroethylene) (ETFE), and fully fluorinated poly(tetrafluoroethene-co-hexafluoropropylene) (FEP) films with subsequent sulfonation to yield cation-exchange sites [8-15], the properties and compositions of the final materials being easily controlled [8,12]. Such proton-exchange membranes have been tested in DMFC mode by Scott *et al.* [16]. Radiation-grafted PVDF-based cation- and anion-exchange membranes have also been applied

to salt-splitting technologies [17-19]; that area would also benefit from this research. Radiation grafting methodology produces ionomer membranes cheaply and has major advantages in that preformed commercial polymer films are modified, alleviating the need for film formation steps, with a wealth of adjustable experimental parameters (*e.g.* radiation dose, temperature, film thickness) allowing a large degree of tailorability. It is essential that the effect of the reaction conditions on the membranes produced is explored in detail for each polymer film / monomer combination [12], which is the basis of this study.

The grafting of vinylbenzyl chloride (VBC) onto FEP (FEP-*g*-PVBC) [20,21] with subsequent amination with trimethylamine and ion-exchange with aqueous potassium hydroxide (FEP-*g*-PVBTMAOH, where VBTMAOH = (vinylbenzyl)trimethylammonium hydroxide) yields alkaline, as opposed to acidic (proton-conducting), membranes (Scheme 1). Preliminary investigations on these types of AAEMs at Surrey [22,23] have demonstrated that PVDF-derived films are not suitable for use in such membranes in alkaline form. This is because the PVDF backbone was shown, by detailed Raman and solid-state NMR studies, to degrade when grafted, aminated and converted to the alkali form. However, these preliminary studies demonstrated that this does not happen with fully fluorinated FEP-derived AAEMs, which retain structural integrity and ion exchange capacity (IEC), even when heated at 60°C for over 2500 h in water [23].

This article follows from our previous work and is concerned with the optimisation of the experimental conditions required to maximise the levels of VBC grafting onto FEP preformed polymer films. A wide range of FEP-*g*-PVBC membranes are

reported (**1** – **17**) and probed using thermogravimetry and Raman microscopy. Selected FEP-*g*-PVBC membranes (**11**, **12**, and **17**) were then aminated and ion-exchanged, to form AAEMs characterised in both the dry and hydrated forms.

2. Experimental

2.1. Chemical supply and pre-treatment

Trimethylamine (Acros Organics, 45% aqueous solution) and toluene (Fisher, specified reagent, low in sulfur) were used as received. Vinylbenzyl chloride (Dow Chemicals, 97%, *m*/*p* ratio of 1.30, stabilised with 75 ppm 4-*t*-butylcatechol and 733 ppm nitromethane, 192 ppm water) was stored in a refrigerator and used without further purification. FEP film (Goodfellow Ltd., U.K. 50 ± 1 μm thickness) was used as received with no pre-wash in any solvent. The standard solutions used for IEC determination were used as received (Aldrich); the potassium hydroxide standards were replaced with fresh solution regularly to reduce the build of carbonate and prevent inaccuracies in the titrations. Deionised water was used throughout this study.

2.2. Polymer film irradiation

The FEP was irradiated with a γ-ray source (Royal Military College, Cranfield University, Shrivenham, U.K) at a temperature of 23 ± 1°C in air. The gamma radiation source consists of twenty rods of ^{60}Co encapsulated in steel tubes in an open cylindrical arrangement. In the shielded position the source is housed in a lead and steel flask incorporating a sliding shutter. The flask is located in a cell of internal dimensions 4 m x 3 m x 3 m. Typical source activity is 146 TBq, giving a maximum dose rate of 12.74 kGy h^{-1}. The total doses for each grafted material are indicated in Table 1. The irradiated films were stored at -30°C in air. During this study, the

materials were used within 1 year of irradiation; radical stability under these storage conditions has been reported previously [8].

2.3. Monomer Grafting to form FEP-*g*-PVBC membranes

A general procedure for the grafting reaction is as follows. The exact reaction conditions for the synthesis of the FEP-*g*-PVBC membranes are given in Table 1. The FEP (known mass) was loosely rolled and immersed in excess vinylbenzyl chloride (or a 50%v/v solution of VBC in toluene) in a cylindrical reaction vessel with a ground glass tap; the VBC was then purged with nitrogen for 2 h at room temperature using a long hollow needle before the tap was closed. The grafting reaction was carried out at 40 - 70°C for known periods of time (days). The grafted membranes were heated at 70°C in toluene overnight to remove any unbound poly(vinylbenzyl chloride) homopolymer and toluene from the membranes was then removed under dynamic vacuum (< 1 mmHg) for > 4 h. FEP-*g*-PVBC membranes (**1** – **17**, Table 1) were obtained as brittle translucent white films, where the degree of grafting (d.o.g.) of the materials were calculated as follows:

$$d.o.g.(\%) = \frac{m_g - m_i}{m_i} \times 100 \qquad (1)$$

where m_g is the grafted mass and m_i is the initial mass of the membranes.

2.4. Amination of selected FEP-*g*-PVBC membranes to form FEP-*g*-PVBTMAOH membranes

Membrane **11** was immersed for 1, 2 and 7 days to establish optimum amination durations (Section 3.3). Membranes **12** and **17** were immersed in a 45% aqueous solution of trimethylamine for 48 h. After amination, the membranes were soaked in deionised water for > 2 h (several changes of water) to remove any excess amine, boiled in water for 1 hour, soaked in water overnight, soaked in excess hydrochloric acid (aq, 1 mol dm^{-3}) for > 48 h (to produce the chloride form), soaked in water for > 48 h with several water changes, and finally stored in water to prevent dehydration. The FEP-*g*-PVBTMAOH membranes **11N**, **12N** and **17N** were generated by immersion in a large excess of potassium hydroxide (aq, 1 mol dm^{-3}) for 48 h followed by immersion in water for > 48 h, with frequent water changes to remove any trapped potassium hydroxide.

2.5. Determination of ion-exchange capacities

Ion-exchange capacities (IECs) were determined as follows. The FEP-*g*-PVBTMAOH membranes were immersed in 20 cm^3 of hydrochloric acid standard (aq, 0.1 mol dm^{-3}) for 48 h. The solutions were then back titrated with potassium hydroxide standard (aq, 0.1 mol dm^{-3}) using a Metrohm 716 DMS Titrino. The titrations were conducted dynamically with a minimum addition of potassium hydroxide of 0.002 cm^3 and a maximum titration rate of 0.5 cm^3 min^{-1}. Endpoints were determined from maxima in the differential titration curves. Three replicates were recorded for each membrane, and a blank run (20 cm^3 of hydrochloric acid (aq, 0.1 mol dm^{-3}) with no membrane) was run alongside each batch to confirm the precision and accuracy of the titrations. The amount of hydroxide anions in the membrane was calculated from the difference between the initial amount of

hydrochloric acid in which the membranes were soaked and the amount of hydrochloric acid remaining (as determined from the titration). After titration the membrane samples are washed in water, soaked in excess hydrochloric acid (aq, 1 mol dm^{-3}) for > 48 h to regenerate the chloride anion forms, soaked in water for > 48 h with frequent changes to remove any trapped acid species, and dried under dynamic vacuum at 80°C (oven). The IECs reported were calculated as below:

$$IEC \quad / \quad eq \quad g^{-1} = \frac{n_i\left(H^+\right) - n_f\left(H^+\right)}{m_{dry}\left(Cl^-\right)} \qquad (2)$$

where $n_i(H^+)$ is the amount of acid the membrane was soaked in, $n_f(H^+)$ is the amount of acid remaining as determined by the titration, and $m_{dry}(Cl^-)$ is the mass of the dried membrane in the chloride-form.

2.6. Water uptake experiments

The FEP-*g*-PVBTMAOH membranes "as-synthesised" (Section 2.4) were first weighed to determine the hydrated mass. The samples were then dried at RH = 0% (in a desiccator over anhydrous calcium chloride) for > 1 week at ambient temperature. It was determined experimentally that this drying methodology gave the same level of drying as treatment in a vacuum oven at 80°C for 4 hours; this low temperature method was adopted for this characterization as it avoids elevated temperatures, which might cause displacement of the trimethylamine functions by the hydroxide anions. The dried masses were recorded and the water uptake was calculated:

$$WU\left(\%\right) = \frac{m_{hyd} - m_{dry}}{m_{dry}} \times 100 \qquad (3)$$

where m_{hyd} is the hydrated mass and m_{dry} is the dry mass. The water uptakes were calculated (average for three membrane segments for each sample) for the hydrated

membranes “as synthesized” and for the membranes after 3 dehydration / rehydration (soaked in water for 24 h) cycles.

2.7. Membrane thicknesses (swelling)

During water uptake experiments, the FEP-*g*-PVBTMAOH membrane thicknesses were measured. These thicknesses (an average of 12 measurements across 3 of membrane segments for each sample) were measured for the hydrated membranes “as synthesised” and the membranes after initial dehydration, rehydration for the third time, and after dehydration for the third time. The thicknesses were recorded using an external micrometer (estimated precision of ±3 μm).

2.8. Thermogravimetry

Thermogravimetry and differential thermal analysis (TG/DTA) were carried out simultaneously in flowing oxygen or nitrogen (60 cm^3 min^{-1}) using a Stanton Redcroft STA-781 thermal analyser. Samples were heated from ambient temperature to 600°C (800°C for the samples analysed in nitrogen) at a heating rate of 2°C min^{-1} (unless otherwise stated). All temperatures quoted in the text are sample temperatures measured with a Pt:Rh(13%) thermocouple in contact with the sample pan. Calcined α-alumina was used as the reference material for DTA, with temperature calibrated from the endotherms arising from the melting of tin or zinc samples. Mass losses arising from evaporation of water were accompanied by endotherms in the DTA traces, while mass losses arising from decomposition of the polymers were accompanied by exotherms. All data were collected on an IBM-compatible computer

with locally written software. The AAEMs were analysed in both the hydrated and dehydrated (RH = 0% for 1 week) states.

2.9. Raman spectroscopy and microscopy

Routine Raman spectra were recorded on a Perkin Elmer System 2000 FT-Raman / near-IR spectrometer with a laser power of 1200 mW and a resolution of 4 cm^{-1}. Liquid and membrane samples were mounted in the beam in glass vials at ambient temperature and pressure.

Raman microscopy was conducted on an Renishaw System 2000 microraman spectrometer with a Ga/Al/As laser (782 nm) generating 13 mW at the sample for the study of graft penetration. The spectra (resolution of 4 cm^{-1}) were recorded with a spatial resolution of a circular area of radius 0.5 μm and a depth of 5 μm. The membrane was pressed between two microscope slides and with the thin edge exposed. The spectra were recorded across the membrane thickness in steps of 2 μm.

3. Results and Discussion

3.1. Studies into the optimisation of the grafting conditions

A series of FEP-*g*-PVBC membranes (**1** – **17**) were synthesised with a variety of irradiation and grafting conditions (Table 1). Figures 1, 2, and 3 show the d.o.g obtained when one grafting parameter is varied at a time (grafting temperature, grafting time, and monomer solution concentration respectively) with films irradiated at both 6.3 and 10 MRad total doses. It is immediately obvious that undiluted VBC, an irradiation total dose of 10 MRad, and a grafting temperature of 50°C yielded membranes with the highest d.o.g; the rate of reaction of the radicals with the vinyl monomer is clearly slow below 50°C, while at temperatures above 50°C the rate of termination by radical combination reactions increases. This result agrees with that found with the grafting of styrene onto ETFE (where the rate of grafting is higher with increasing temperature, but the rate of radical termination also increases above 50°C leading to lower actual saturation grafting levels [12]). Increased total dose leads to increased d.o.g. as expected. Total doses above 10 MRad for FEP lead to base polymer embrittlement, which is not desirable. The variation with grafting time is not clear-cut but 48 h appears sufficient (longer grafting times than this appear not to have a significant effect on the level of grafting).

3.2. Thermogravimetry of the FEP-*g*-PVBC membranes in oxygen

Oxygen was initially selected for the atmosphere required for thermogravimetry as this would give the harshest regime for thermal analysis and also because oxygen is

present in the operation of fuel cells (an intended application). The TG/DTA trace of the pre-irradiated FEP film in oxygen is shown in Figure 4. The decomposition in oxygen of FEP commences at 403°C and proceeds rapidly in a two-stage process; exotherms were associated with both of these two stages. Less than 2% mass remained at 600°C. TGA/DTA analysis was conducted on most of the FEP-*g*-PVBC membranes synthesised (**11** and **12** were required for amination studies and so were not studied). A typical example is shown in Figure 5, which shows the combined TG and DTA data recorded with membrane **17**, with the features of importance highlighted. Particular points of interest for the FEP-*g*-PVBC membranes are the temperature at which decomposition commences and the magnitude of the *first mass loss*; in membranes of higher d.o.g., this first mass loss appeared to proceed in two stages, but these are considered as one in the following discussion as the stages cannot be resolved. The presence of two distinct degradation stages indicates the formation of FEP / poly(VBC) phase separated microdomains, similar to that previously reported for styrene grafted FEP materials [24].

For membrane **17** (28.9% d.o.g.), decomposition in oxygen commenced at 222°C (a significant drop in short-term stability in oxygen compared with FEP) and a first mass loss of 14.9% was observed. This first mass loss is much lower than the 28.9 % expected if this mass loss was the complete loss of grafted hydrocarbon component. This pattern was observed for all the FEP-*g*-PVBC membranes studied and suggests that the decomposition of organic components overlap with the decomposition of the fluoropolymer backbones and also that a significant fraction of aromatic content remains at elevated temperatures [24,25]. The first mass loss was associated with two small exotherms (confirming this mass loss as a two stage process); the second mass

Deleted: 4

loss (the largest with a magnitude of 82.9% and predominantly due to loss of the fluorocarbon backbone) appeared to proceed in a single stage and this is confirmed by a single associated exotherm. With FEP-*g*-PVBC membranes of low d.o.g. (*e.g.* **15**), this second mass loss was larger in magnitude and approached the behaviour observed for FEP *i.e* a two stage decomposition with two associated exotherms.

There was no evidence in the TG traces of any trapped unbound VBC in any of the membranes, which would have manifested itself as low temperature mass losses with associated endotherms in DTA traces (evaporation of the monomer). Figure 6 presents the combined data from all the TG traces collected and shows the relationship between the magnitude of the first mass loss and the decomposition onset temperature with respect to the degrees of grafting of the membranes. A spread of data was observed, but linear relationships were apparent. This spread of data may originate from variations in morphology of the materials (*i.e.* the level mixing between the hydrocarbon graft domains and the FEP fluoropolymer rich domains may vary with the grafting conditions). The lower the d.o.g. the lower is the magnitude of the first mass loss. There was also a small drop in apparent short-term thermal stability with increasing d.o.g. (increasing hydrocarbon component). This may be an artefact of the "observability" of the onset point for decomposition; the higher the graft loading, the easier decomposition is to spot. As previously reported by Scherer *et al*. [25] in the study of sulfonated styrene grafted FEP membranes, TG data do not give accurate indication of long-term thermal stabilities; the decomposition occurs slowly at lower temperatures and this is easily masked by the relatively fast heating rates. Long-term (> 1 year) stability testing in water at 50°C (monitoring the IEC with time) is now

being conducted for **12N** and will be reported in due course (so far after > 100 days, > 87% of the original IEC remains).

3.3 Raman spectroscopy of the FEP-*g*-PVBC membranes

The Raman spectrum of FEP (Figure 7) shows bands that have been previously observed for PTFE [26]. The bands observed are (cm^{-1}): 1381*m* ν_s(C-C), 1300*m* ν(C-C), 1216*w* ν_{as}(C-C), 734*s* $\nu_s(CF_2)$ with a shoulder at 752*m* which is not observed for PTFE, 598*w* $\delta(CF_2)$, 579*w* $\delta(CF_2)$, 387*m* $\delta(CF_2)$, and 292*m* $t(CF_2)$.

The above FEP bands are all present in the Raman spectrum of **17N** (Figure 7). New bands are observed, also present in the Raman spectrum of poly(vinylbenzyl chloride). The most significant of new bands are located at (cm^{-1}): 1613*s* (aromatic ring breathing), 1268*s* (CH_2Cl), and 1002*s* (the ν_{12} band in the spectrum of poly(styrene) [27]). The absence of a band at 1632 cm^{-1} (the strong C=C band located in the Raman spectrum of VBC) confirms that no residual VBC monomer remains in the membranes (corroborating TG data where no low temperature mass loss or endotherm assignable to evaporation of VBC was observed). The intensities of the poly(vinylbenzyl chloride) bands are directly related to the degree of grafting, with **17** exhibiting the most intense bands.

3.4 The study of graft penetration using Raman microscopy

Raman microscopy was used to measure the graft penetration of the VBC component within the thickness of the FEP base film, as has been previously reported for PFA-

styrene radiation grafted systems [28,29] (PFA = poly(tetrafluoroethylene-*co*-perfluoropropylvinyl ether)). The intensity of the strong ring-breathing band of the poly(vinylbenzyl chloride) component at 1002 cm^{-1} compared to the intensity of the FEP band at 387 cm^{-1} was recorded at 2 μm steps across the thickness of selected FEP-*g*-PVBC membranes (Figure 8). These bands were selected as they were determined to be single bands which were well separated from nearby bands. Information that was obtained from these data was: (a) the level of grafting from the magnitude of the ratio of band intensities, and (b) the variation in grafting levels at different positions within the membranes.

From Figure 8 it can be seen that membrane **16** (with a low d.o.g. o= 6.4%) showed a significant drop of VBC component within the membrane interior compared with the edges. In contrast, membrane **17** with the highest d.o.g. obtained in this study of 28.9% showed a reasonably high and uniform level of VBC component throughout the thickness of the membrane. Figure 8 clearly shows that the amount of VBC component within the membrane increases with an increasing d.o.g. for each of the membranes studied. The cross section is quite "noisy", indicating some fluctuations in the amount of each component throughout the membrane thickness; this is consistent with previously proposed microdomains [24]. For some of the membranes, there is a sudden increase in the level of VBC component at the membrane surfaces; this indicates surface-grafted VBC homopolymer.

3.5. Amination of 11 for optimisation of amination times

Membrane **11** was aminated and ion-exchanged to form the AAEM **11N** for the purpose of studying the effect of amination time on the IECs of the membranes produced. Amination times of 1, 2 and 7 days were studied. It was evident that amination times > 1 day made very little difference on the IECs: IEC(1 day) = 0.99 meq g^{-1}, IEC(2 day) = 1.00 meq g^{-1}, and IEC(7 day) = 0.96 meq g^{-1} (arithmetic mean = 0.98 μm, standard deviation 0.02 μm). Amination times of 48 h were used for subsequent amination reactions.

Deleted: ton

3.6. Ion-exchange capacities (IECs) of 11N, 12N and 17N AAEMs

The IECs increase with increasing degree of grafting as expected (Table 2); the highest exchange capacity obtained was 1.08 meg g^{-1} for **17N**, which is higher than that found with the Nafion®-11x series of membranes (0.92 meq g^{-1}). The values determined by titration (Table 2) were lower than the maximum theoretical values that were calculated when assuming 100% amination, 100% water removal on drying, and no side-reactions (the experimental values were between 65 – 80% of the calculated values). This indicates: (a) displacement of a minor number of NMe_3 groups on treatment with potassium hydroxide (1 mol dm^{-3}), or (b) incomplete amination, or (c) incomplete dehydration. Raman spectroscopic investigations (Section 3.9) confirm complete amination and (b) above can be discounted. The TG of dried **17N** in the chloride form (post titration) showed that 5% of the mass was due to water, hence, the corrected IEC would be 1.14 meq g^{-1} for a dried membrane containing no traces of water.

3.7 Water uptake and variation in thickness of 12N and 17N

The water uptakes "as-synthesised" and after 3 dehydration / rehydration cycles for **12N** and **17N** show that the membranes with higher degrees of grafting (and IEC) absorbed more water (as expected). The water uptakes were higher initially as the synthesis of the AAEMs involved boiling step (after treatment in trimethylamine) which would have expanded the membrane to the maximum extent; the dehydration / rehydration cycles (in the alkaline form) involved no such process, as hydration consisted of immersion in water for 24 h.

17N also showed slightly increased thicknesses compared with **12N**, as expected and for both hydration states (Table 2). The thicknesses of both hydrated membranes were larger "as-synthesised" (Section 2.4) than after the dehydration / rehydration cycles, mirroring water uptake observations. However, the thickness of dehydrated **17N** after the dehydration / rehydration cycles was larger than when the thickness was measured after initial dehydration; this was not expected and may indicate that repeated dehydration / rehydration affects the morphology of the AAEMs. The thickness of **17N** after initial dehydration (62 μm) was also observed to be smaller than the thickness of the pre-aminated grafted membrane **17** (65 μm); if anything a small increase in thickness had been expected with the introduction of bulkier trimethylammonium hydroxide groups replacing the chloride atoms of the benzylchloride functions in **17**. The above observations on thicknesses, however, must be considered in perspective; the difference in thicknesses between **12N** and **17N** in the same hydration state was sometimes within the resolution window (± 3 μm). Also, from the standard deviations it can be seen that there was a spread of

thicknesses for each AAEM in each hydration state, which suggests some variation of the level of grafting across the area of each membrane.

3.8 Thermogravimetry of the AAEMs 12N and 17N

The TG/DTA curves of AAEMs **12N** and **17N** were recorded in oxygen for both the hydrated and dry (RH = 0% for 1 week) states (Table 3); the heating rate for the aminated samples was changed to 5°C min^{-1} (dpm) to allow the data for the hydrated and dehydrated samples for each material to be collected on the same day. The TG curves recorded in oxygen for FEP, **17** and **17N** (hydrated and dry states) are presented in Figure 9 to aid visualisation of the discussions below.

An initial mass loss (30 – 164°C, associated endotherm) was observed with the AAEMs in both hydration states and corresponds to loss of water. This initial mass loss was larger for both of the hydrated AAEMs compared to the dehydrated AAEMs as expected; however the magnitude of these initial mass losses (31.2% and 30.2% for hydrated **12N** and **17N** respectively) were much lower than the corresponding water uptakes (Section 3.7, Table 2). Therefore, some loss of water must either overlap with (or mechanistically contribute to) material decomposition, resulting in complications in the quantitative analysis.

Deleted: The TG study of these materials was repeated in nitrogen; the use of an inert atmosphere could delay the onset of material decomposition (resulting in improved resolution between this and loss of water content) but this was not the case (Table 3, Figure 10).

Water loss was also evident on heating dehydrated **12N** and **17N** (the corresponding initial mass losses in the range 30 - 154°C were 4.0% and 6.8% respectively). This indicates drying at RH = 0% (in a desiccator over anhydrous calcium chloride) for 1 week does not remove all of the water content for the AAEMs. This was anticipated,

as the OH^- ions would form strong hydrogen bonds to water resulting in a strongly bound hydration sphere. The material with the larger IEC retained the most water on dehydration, as expected.

A second mass loss occurs at begins at 151 – 165°C (Table 3) for both **12N** and **17N** in all humidity states in oxygen (with associated exotherms). This mass loss is due to the onset of polymer degradation through the loss of amine species; the state of hydration or the original degree of grafting does not significantly affect the inherent short-term stability of the AAEMs. All further higher temperature mass losses observed relate directly to the mass losses observed for the degradation of pre-aminated grafted FEP-*g*-PVCBC membranes (Section 3.2).

Deleted: 15N

The TG study of these materials was repeated in nitrogen; the use of an inert atmosphere could delay the onset of material decomposition (resulting in improved resolution between this and loss of water content) but this was not the case (Table 3, Figure 10).

3.9 Raman spectroscopy of FEP-*g*-PVBTMAOH AAEMs

The Raman spectra of **17N** (wet and dry) and vinylbenzyltrimethylammonium chloride for comparison are shown in Figure 7. The bands at 1267*s* (CH_2Cl), 1185*m*, 834*m*, 712*m*, 700*m*, and 683*m* cm^{-1} that were present in the Raman spectrum of **17** disappear on amination to **17N**; the lack of these bands indicates complete amination. New bands at 1454*m*, 1064*w*, 978*w*, 893*w*, and 754*m* cm^{-1} are observed; these bands are also present in the Raman spectrum of vinylbenzyltrimethylammonium chloride.

There was very little difference between the spectra of dry and wet **17N** with only a small decrease in the signal to noise ratio for the wet sample.

In Section 3.6 the lower than expected IECs may have arisen from displacement of the ammonium groups by the OH^- ions required for conversion to the alkaline-form AEM. This would lead to CH_2OH groups attached to the aromatic rings. The Raman spectrum of vinylbenzyl alcohol (not shown) contains bands at 1310*m*, 1180*m*, and 827*m* cm^{-1} that are not present in the Raman spectra of vinylbenzyl chloride and vinylbenzyltrimethylammonium chloride. These bands are also not observed in Raman spectra of dry **17N**; this nucleophillic displacement of amine by hydroxide ions is minimal and will in future allow the IECs of the anion-exchange membranes to be measured directly for the alkaline, as opposed to the chloride, forms. OH^- has a molecular mass (17.0 g mol^{-1}) that is lower than Cl^- (35.5 g mol^{-1}), and hence the IECs of hydroxide-form membranes will be higher than the analogous chloride forms (*e.g.* for membrane **11N**, the theoretical maximum value for the IEC of the hydroxide form is 1.32 meq g^{-1} while the calculated IEC for the chloride form is 1.22 meq g^{-1}); this means that the IECs reported in this study are lower than the true IECs of the AAEMs synthesised.

Deleted: n

Deleted: This

3.10 Preliminary conductivity measurements

Two probe impedance spectroscopy on membranes **12N** and **17N** (recorded on a Solartron 1260 Frequency Response Analyser / 1287 Electrochemical Interface combination with frequencies between 1 Hz and 1 MHz and a 10 mV a.c. voltage amplitude and using the method which has been previously reported [23]) gave proton

conductivities of around 0.01 S cm^{-1} for both membranes. This is a satisfactory order of magnitude for application in fuel cells.

Formatted

4. Conclusions

The following conclusions relate to use of 50 ± 1 μm thick poly(hexafluoropropylene-co-tetrafluoroethylene) polymer (FEP, Goodfellow) as a precursor film and the monomer vinylbenzyl chloride (VBC, Dow Chemicals). Trimethylamine (aq, 45%mass) and KOH (aq, 1 mol dm^{-3}) were used for conversion to alkaline anion-exchange membranes.

(1) Vinylbenzyl chloride (VBC) can been successfully pre-irradiation grafted onto FEP to yield FEP-*g*-PVBC membranes (**1** – **17**) with degrees of grafting in the range of 3.3 – 28.9%.

(2) Optimum grafting conditions (for maximum degrees of grafting) were determined as irradiated film immersion in undiluted VBC at 50°C for 48 hours. Higher irradiation total doses give higher degrees of grafting.

(3) The short-term thermal stabilities of the FEP-*g*-PVBC membranes (determined by thermogravimetry) reduce slightly with increasing levels of grafting.

(4) The graft penetration improved with increasing degree of grafting. There is no evidence of any trapped and unbound VBC in the grafted materials.

(6) Selected FEP-*g*-PVBC membranes were successfully aminated with trimethylamine and ion-exchanged with aqueous potassium hydroxide to give benzyltrimethylammonium hydroxide alkaline anion-exchange membranes (**11N**, **12N**, and **17N**).

(7) Optimisation studies indicate that amination times of 48 h at room temperature are adequate.

(8) The ion-exchange capacities, water uptakes, and membrane swelling (thickness) generally increase with increasing d.o.g.

(9) Thermogravimetry of alkaline anion-exchange membranes of this type is not sufficient for determination of water uptakes.

(10) The onset of degradation of the final alkaline anion-exchange membranes does not depend on the degree of grafting or the membrane humidity.

(11) Raman spectroscopic studies confirm complete amination of the FEP-*g*-PVBC membranes with minimal nucleophillic displacement of amine by the OH^- ions in the ion-exchange reaction.

The AAEMs produced in this study are currently being evaluated in a direct methanol fuel cell; the performance curves (along with data on *in-situ* membrane resistivities and stabilities) will be reported at a later date.

Deleted: The AAEMs produced in this study are currently being evaluated for fuel cell application, and associated performances, membrane conductivities, and in-situ membrane stability data will be published in due course.

Formatted

Acknowledgments

The authors gratefully thank Keith Lovell of the Royal Military College Shrivenham, Cranfield University for the irradiation of the FEP films and for useful discussions.

References

1 H. F. Gibbard, Batteries versus Fuel Cells: The Application of a Disruptive Technology, EyesforFuelCells Conference on Fuel Cells for Portable Applications, Boston, USA, September (2002).

2 A. K. Shukla, C. L. Jackson, K. Scott, R. K. Raman, An improved-performance liquid-feed solid-polymer-electrolyte direct methanol fuel cell operating at near-ambient conditions, Electrochim. Acta, 47 (2002) 3401.

3 B. Gurau, E. S. Smotkin, Methanol crossover in direct methanol fuel cells: a link between power and energy density, J. Power Sources, 112 (2002) 339.

4 J. A. Kerres, Development of ionomer membranes for fuel cells, J. Membr. Sci., 185 (2001) 3.

5 D. Chu, R. Jiang, Novel electrocatalysts for direct methanol fuel cells, Solid State Ionics, 148 (2002) 591.

6 D. R. Thomas, X. Ren, S. Gottesfeld, P. Zelenay, Direct methanol fuel cells: progress in cell performance and cathode research, Electrochim. Acta, 47 (2002) 3741.

7 G. F. McLean, T. Niet, S. Prince-Richard, N. Djilali, An assesment of alkaline fuel cell technology, Int. J. Hydrogen Energy, 27 (2002) 507.

8 K. V. Lovell, J. A. Horsfall, Synthesis and characterisation of sulfonic acid-containing ion exchange membranes based on hydrocarbon and fluorocarbon polymers, Eur. Polym. J., 38 (2002) 1671.

9 J. A. Horsfall, K. V. Lovell, Fuel cell performance of radiation-grafted sulfonic acid membranes, Fuel Cells, 1 (2001) 186.

10 J. A. Horsfall, K. V. Lovell, Comparison of fuel cell performance of selected fluoropolymer and hydrocarbon based grafted copolymers incorporating acrylic acid and styrene sulfonic acid, Polym. Adv. Tech., 13 (2002) 381.

11 C. Chuy, V. I. Basura, E. Simon, S. Holdcroft, J. A. Horsfall, K. V. Lovell, Electrochemical characterisation of ethylenetetrafluoroethylene-g-polystyrenesulfonic acid solid polymer electrolytes, J. Electrochem. Soc., 147 (2000) 4453.

12 P. Brack, H. G. Buhrer, L. Bonorand, G. G. Scherer, Grafting of pre-irradiated poly(ethylene-alt-tetrafluoroethylene) films with styrene: influence of base polymer film properties and processing parameters, J. Mater. Chem., 10 (2000) 1795.

13 S. Hietala, S. L. Maunu, F. Sundholm, T. Lehtinen, G. Sundholm, Water sorption and diffusion coefficients of protons and water in PVDF-g-PSSA polymer electrolyte membranes, J. Polym. Sci. : Part B: Polym. Phys., 37 (1999) 2893.

14 J. A. Horsfall, K. V. Lovell, Synthesis and characterisation of acrylic acid-grafted hydrocarbon and fluorocarbon polymers with the simultaneous or mutual grafting technique, J. Appl. Polym. Sci., 87 (2003) 230.

15 S. D. Flint, R. C. T. Slade, Investigation of radiation-Grafted PVDF-g-polystyrene-sulfonic-acid ion exchange membranes for use in hydrogen oxygen fuel cells, Solid State Ionics, 97 (1997) 299.

16 K. Scott, W. M. Taama, P. Argyropoulos, Performance of direct methanol fuel cell with radiation-grafted polymer membranes, J. Membr. Sci., 171 (2000) 119.

17 N. Tzanetakis, W. M. Taama, K. Scott, J. R. Varcoe, R. C. T. Slade, Salt splitting with radiation grafted PVDF membranes, Desalination, 151 (2002) 275.

18 N. Tzanetakis, W. M. Taama, K. Scott, R. J. J. Jachuck, R. C. T. Slade, J. R. Varcoe, Comparative performance of ion exchange membranes for electrodialysis of nickel and cobalt, Sep. Puri. Tech., 30 (2003) 113.

19 N. Tzanetakis, J. R. Varcoe, R. C. T. Slade, K. Scott, Salt splitting with radiation grafted PVDF anion-exchange membrane, Electrochem. Commun., 5 (2003) 115.

20 J. Sandeaus, R. Sandeaus, G. Pourcelly, J. Molénat, Desorption of counter-ions followed with labelled ions and water dissociation in perfluorinated quaternary ammonium membranes and Nafion-125 membranes, J. Membr. Sci., 84 (1993) 213.

21 T. Cohen, P. Dagard, J. Molénat, B. Brun, C. Gavach, Proton leakage through pefluorinated anion exchange membranes, J. Electroanal. Chem., 210 (1986) 329.

22 T. N. Danks, R. C. T. Slade, J. R. Varcoe, Comparison of PVDF- and FEP-based radiation-grafted alkaline anion-exchange membranes for use in low temperature portable DMFCs, J. Mater. Chem., 12 (2002) 3371.

23 T. N. Danks, R. C. T. Slade, J. R. Varcoe, Alkaline anion-exchange radiation-grafted membranes for possible electrochemical application in fuel cells, J. Mater. Chem., 13 (2003) 712.

24 M. M. Nasef, H. Saidi, Thermal degradation behaviour of radiation grafted FEP-g-polystyrene sulfonic acid membranes, Polym. Degrad. Stab., 70 (2000) 497.

25 B. Gupta, G. G. Scherer, Proton exchange membranes by radiation grafting of styrene onto FEP films. I. Thermal characteristics of copolymer membranes, J. Appl. Chem. USSR, 50 (1993) 2129.

26 A. Gruger, A. Régis, T. Schmatko, P. Colomban, Nanostructure of Nafion® membranes at different states of hydration. An IR and Raman study, Vibr. Spectrosc., 26 (2001) 215.

27 B. Jasse, R. S. Chao, J. L. Koenig, Laser raman scattering in uniaxially orientated atactic polystyrene, J. Polym. Sci.: Polym. Phys. Ed., 16 (1978) 2157.

28 F. Cardona, G. A. George, D. J. T. Hill, F. Rasoul, J. Maeji, Copolymers obtained by the radiation-induced grafting of styrene onto poly(tetrafluoroethylene-co-

Deleted: x

Deleted: Accepted and in-press.

perfluoropropylvinyl ether) substrates. 1. Preparation and structural investigation, Macromolecules, 35 (2002) 355.

29 F. Cardona, G. A. George, D. J. T. Hill, S. Perera, Spectroscopic study of the penetration depth of grafted polystyrene onto poly(tetrafluoroethylene-co-perfluoropropylvinylether) substrates. 1. Effect of grafting conditions, J. Polym. Sci.: Part A: Polym. Chem., 40 (2002) 3191.

Scheme 1: Preparation of FEP-*g*-PVBC radiation grafted membranes from FEP and vinylbenzyl chloride. Subsequent amination and ion-exchange yields the benzyltrimethylammonium hydroxide alkaline anion-exchange membranes (AAEMs) analogues (FEP-*g*-PVBTMAOH).

Figure 1: The effect of grafting temperature on the d.o.g. of the membranes synthesised using FEP films irradiated with total doses of 6.3 MRad (•) and 10 MRad (o). Neat VBC was used, with grafting periods of 24 h.

Figure 2: The effect of grafting times on the d.o.g. of the membranes synthesised using FEP films irradiated with total doses of 6.3 MRad (•) and 10 MRad (o). Neat VBC was used, with a monomer solution temperature of 60°C.

Figure 3: The effect of VBC concentration on the d.o.g. of the membranes synthesised using FEP films irradiated with total doses of 6.3 MRad (•) and 10 MRad (o). Immersion times of 24 h were used, with a monomer solution temperature of 60°C.

Figure 4: The TG / DTA trace of FEP recorded in flowing oxygen (60 cm^3 min^{-1}) with a heating rate of 2°C min^{-1} over the range 30 - 600°C.

Figure 5: The TG / DTA trace of **17** (28.9% d.o.g., Table 1) recorded in flowing oxygen (60 cm^3 min^{-1}) with a heating rate of 2°C min^{-1} over the range 30 - 600°C. The extent of the first mass loss (corresponding to loss of some of the hydrocarbon component) is between the horizontal parallel lines; this mass loss region is referred to throughout this text.

Figure 6: A plot of the onset temperatures for the first mass loss (•) and the magnitude of this first mass loss (o) versus the degree of grafting for the FEP-*g*-PVBC membranes (see Figure 5 for definitions). The squares indicate the membranes selected for Raman microscopic study.

Figure 7: The Raman spectra of: (a) FEP, (b) vinylbenzyl chloride (liquid, as purchased), (c) membrane **17**, (d) membrane **17N** when dry, (e) membrane **17N** when wet, and (f) vinylbenzyltrimethylammonium chloride (powder).

Figure 8: Raman microscopic measurement of the ratio of intensities of the benzyl chloride ring breathing band at 1002 cm^{-1} to the FEP band at 387 cm^{-1} at 2 μm steps across the thickness of selected FEP-*g*-PVBC membranes. Figures in square brackets are the [degree of grafting].

Figure 9: The TG curves (in oxygen) of: (a) FEP, (b) membrane **17**, (c) dehydrated AAEM **17N**, and (d) hydrated AAEM **17N**.

Figure 10: The TG curves (in nitrogen) of: (a) membrane **17**, (b) dehydrated AAEM **17N**, and (c) hydrated AAEM **17N**.

Membrane	Total dose / MRad	Grafting temp. / °C	Immersion time / h	Monomer conc. (%v/v)	*d.o.g (%)*
1	6.3	70	24	100	*15.2*
2	10	70	24	100	*21.3*
3	10	60	24	100	*24.4*
4	10	60	24	100	*24.9*
5	6.3	60	48	100	*23.4*
6	10	60	48	100	*26.4*
7	6.3	60	24	100	*17.7*
8	10	60	24	100	*23.1*
9	6.3	60	24	50	*10.7*
10	10	60	24	50	*12.6*
11	10	60	96	100	*25.2*
12	10	60	93	100	*24.3*
13	6.3	50	24	100	*24.7*
14	10	50	24	100	*28.0*
15	6.3	40	24	100	*3.3*
16	10	40	24	100	*6.4*
17	10	50	72	100	*28.9*

Table 1: The irradiation and grafting for the FEP-*g*-PVBC materials synthesised giving the total dose of γ-radiation used, the time and temperature of immersion of the irradiated films in the monomer solution, and the concentration of monomer solution (either neat VBC (100%v/v or VBC dissolved in toluene (50%v/v)). d.o.g. is the degree of grafting of the resulting materials (see Equation 1).

Membrane *[d.o.g.(%)]*	**IEC_{obs} / meq g^{-1}**	**IEC_{calc} / meq g^{-1}**	**WU_{ini} (%)**	**WU_{3rd} (%)**	***t_{hi}* / μm**	***t_{d1}* / μm**	***t_{h3}* / μm**	***t_{d3}* / μm**
11N	0.98	1.22	-	-	-	-	-	-
[25.2]	(0.02)							
12N	0.77	1.19	48.2	38.8	86	62	79	63
[24.3]	(0.01)		(2.7)	(1.2)	(3.5)	(1.3)	(5.4)	(2.1)
17N	1.08	1.35	54.4	41.0	88	62	82	66
[28.9]	(0.02)		(1.9)	(1.0)	(2.6)	(1.6)	(3.4)	(2.1)

Table 2: Combined data for the FEP-*g*-PVBTMAOH AAEMs. Figures in brackets are the sample standard deviations with replicate measurements. IEC_{obs} is the observed IECs. IEC_{calc} is the theoretical maximum IECs calculated from the d.o.g. assuming 100% amination, 100% water removal on drying, and no side-reactions. WU_{ini} is the initial water uptake and WU_{3rd} is the water uptake determined after 3 dehydration / rehydration cycles. t_{hi} is the thickness of the hydrated membranes "as synthesised", t_{d1} is the thickness of the membranes on first dehydration, t_{h3} is the thickness on the third rehydration, and t_{d3} is the thickness on the third dehydration. For comparison, the thickness of FEP-*g*-PVBC membrane **17** was 65 (0.5) μm.

AAEM	Atmosphere	Humidity State	Magnitude of 1st mass loss (%)	Onset of 2nd mass loss (°C)	Magnitude of 2nd mass loss (%)
12N	oxygen	wet	31.2	164	5.1
[24.3%]	oxygen	dry	4.0	154	9.6
	oxygen	wet	30.2	156	7.0
17N	oxygen	dry	6.8	151	10.7
[28.9%]	nitrogen	wet	31.2	165	5.0
	nitrogen	dry	2.0	136	12.7

Table 3: Selected thermogravimetry data for AAEMs **12N** and **17N** (Figures 9 and 10). The first mass loss is associated with loss of water content, while the second mass loss is due to the first stage of polymer degradation. Figures in square brackets are the [d.o.g.].

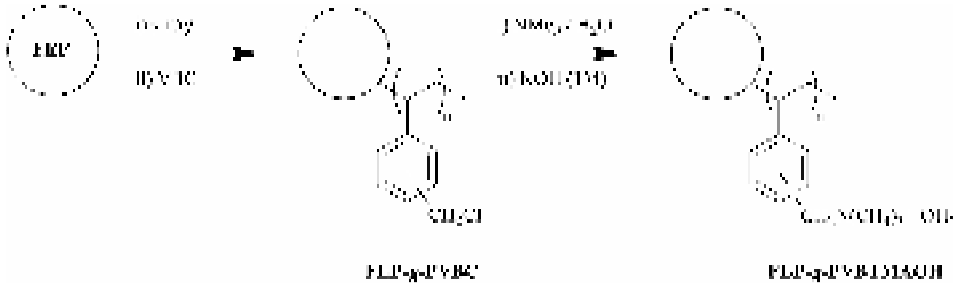

Scheme 1

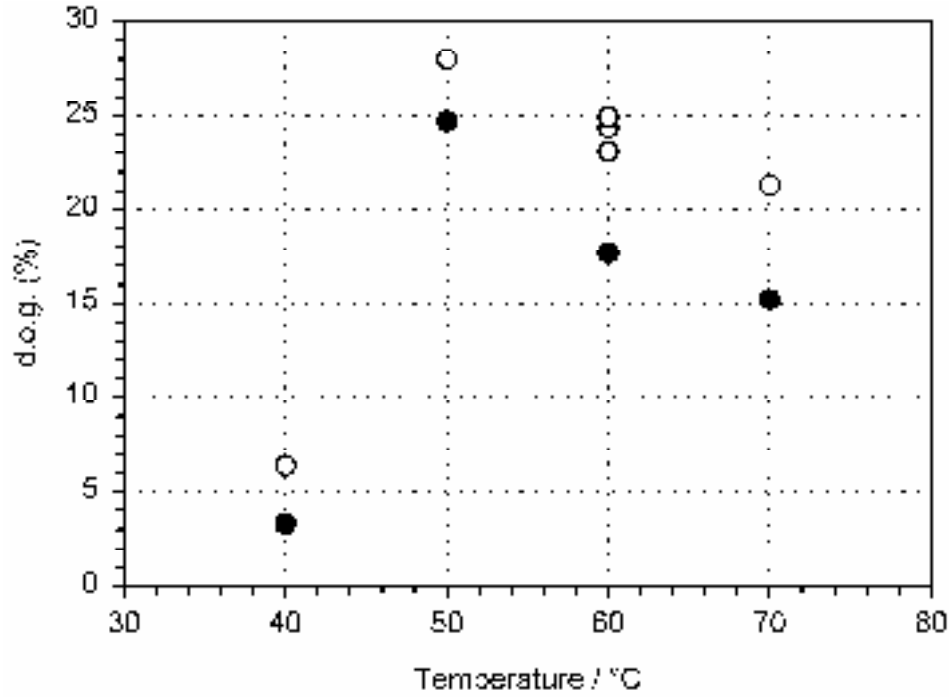

Figure 1

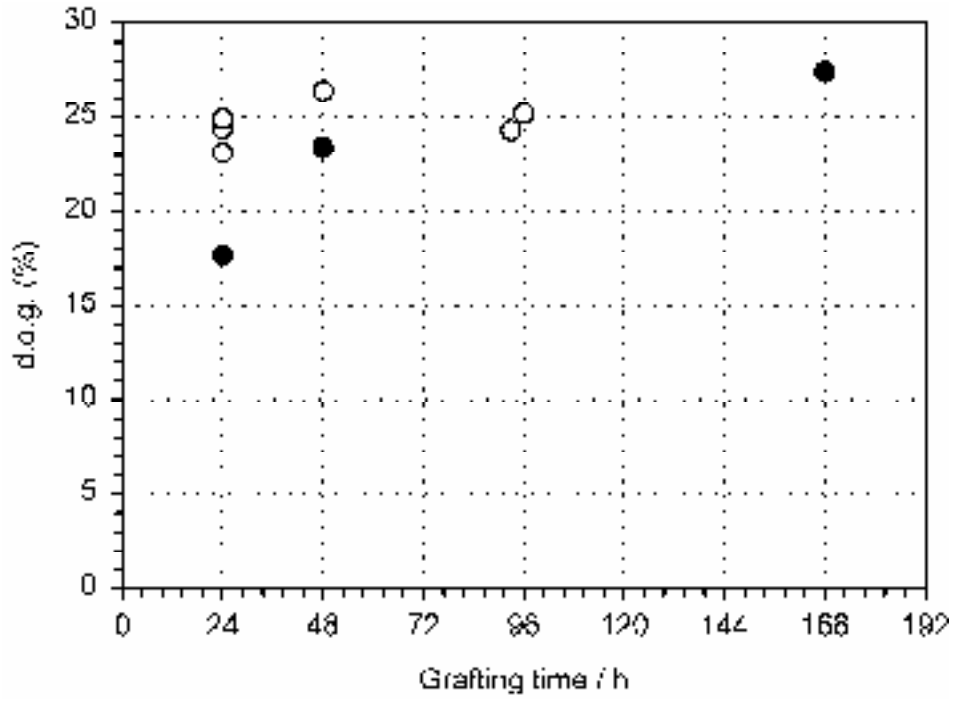

Figure 2

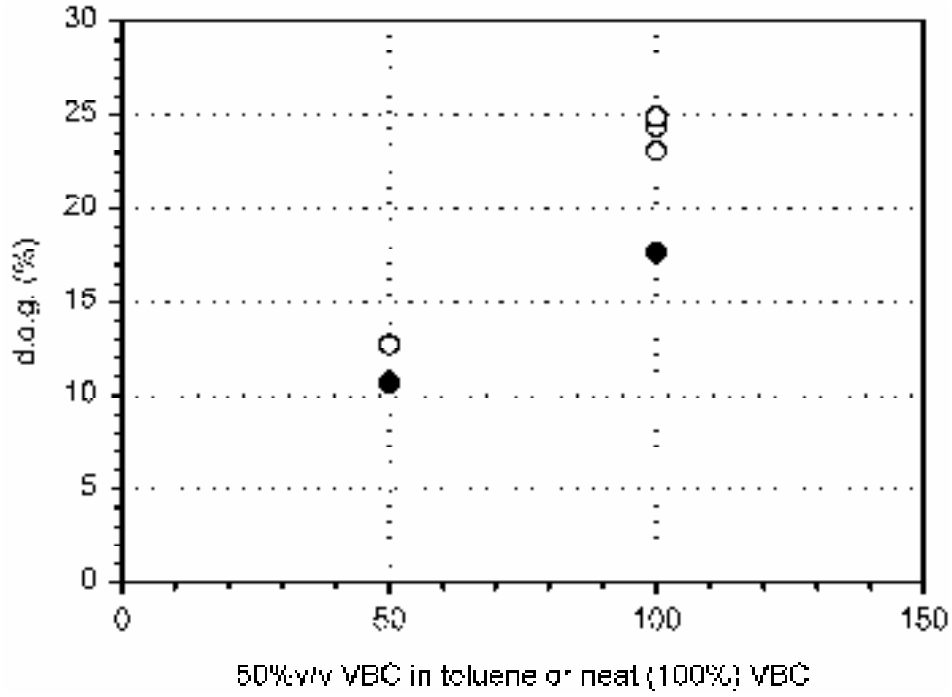
30
25
20
15
10
5
0
d.o.g. (%)
0
50
100
150
50%v/v VBC in toluene or neat (100%) VBC

Figure 3

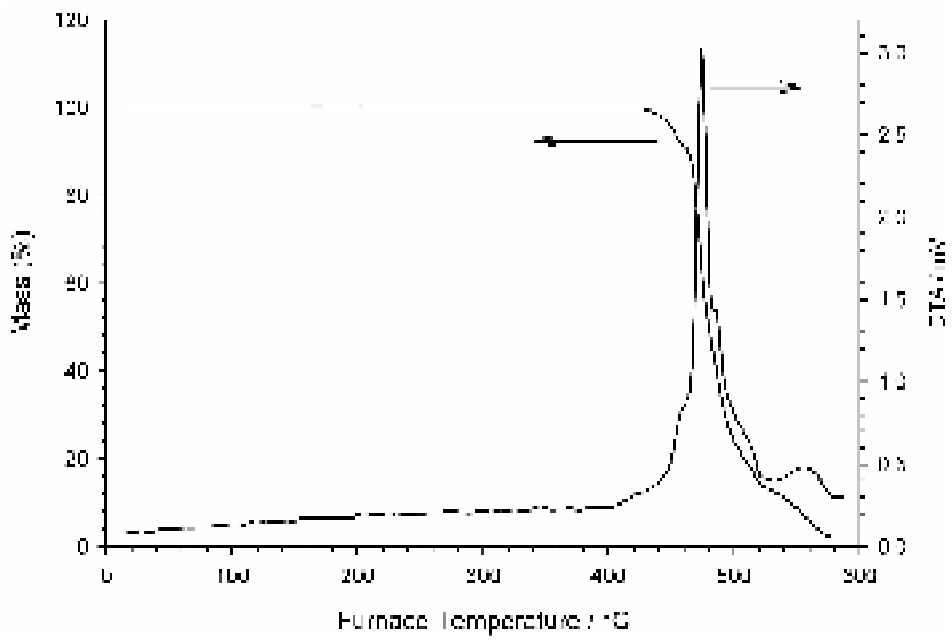

Figure 4

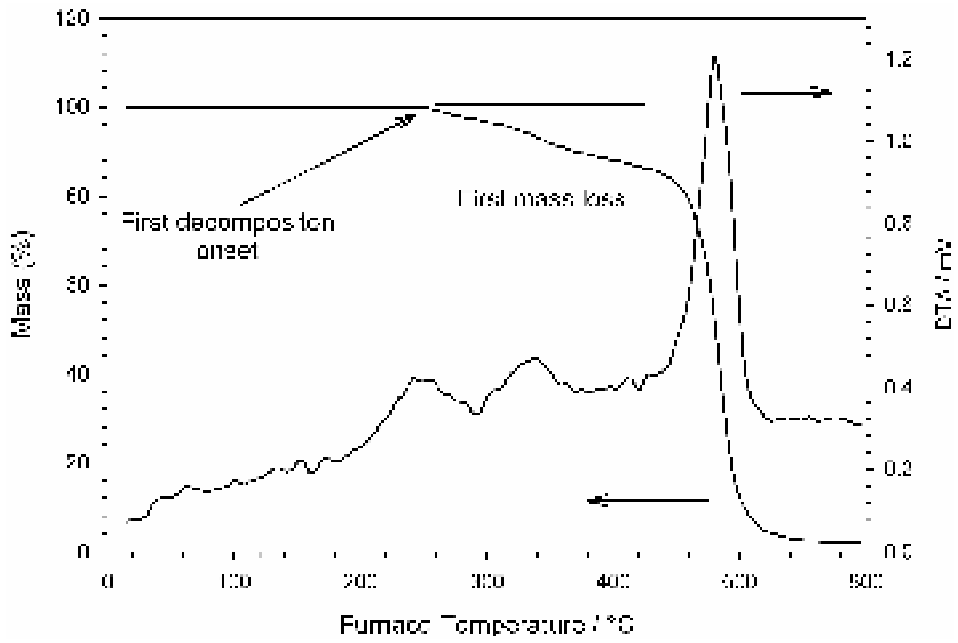
120
100
80
60
40
20
0
Mass (%)
First decomposition onset
First mass loss
1.2
1.0
0.8
0.6
0.4
0.2
0.0
DTA / mV
0
100
200
300
400
500
Furnace Temperature / °C

Figure 5

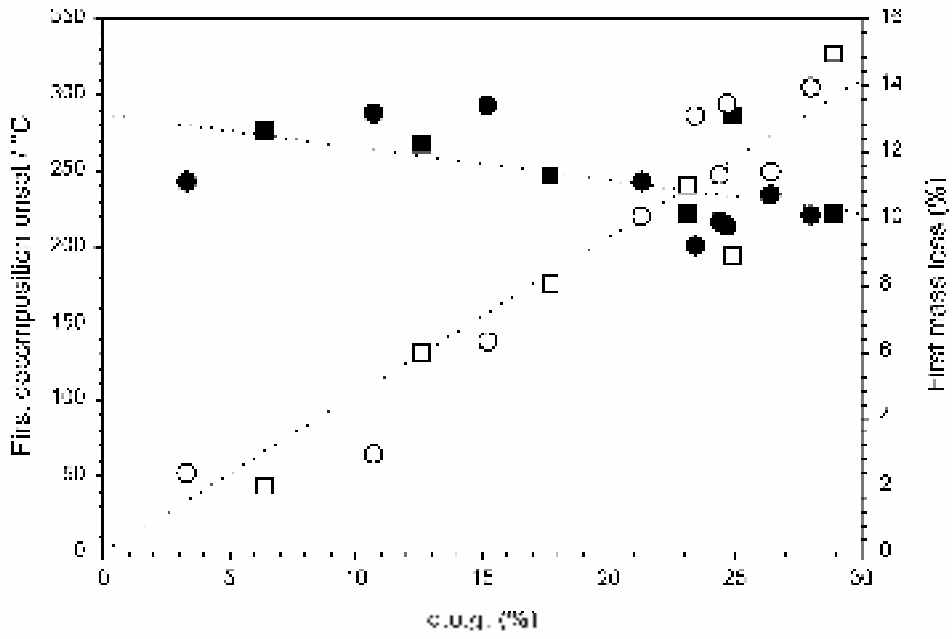

Figure 6

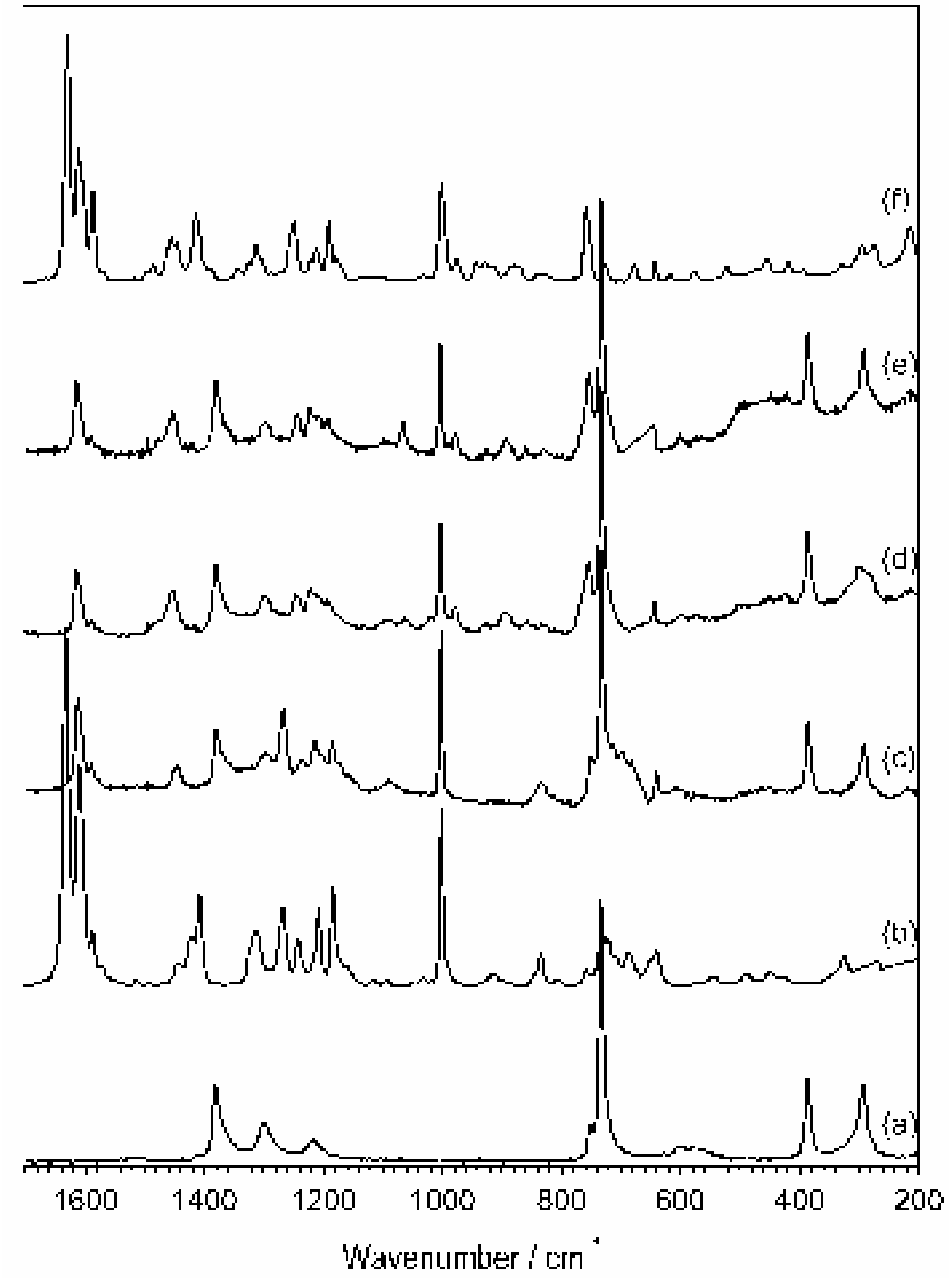

Figure 7

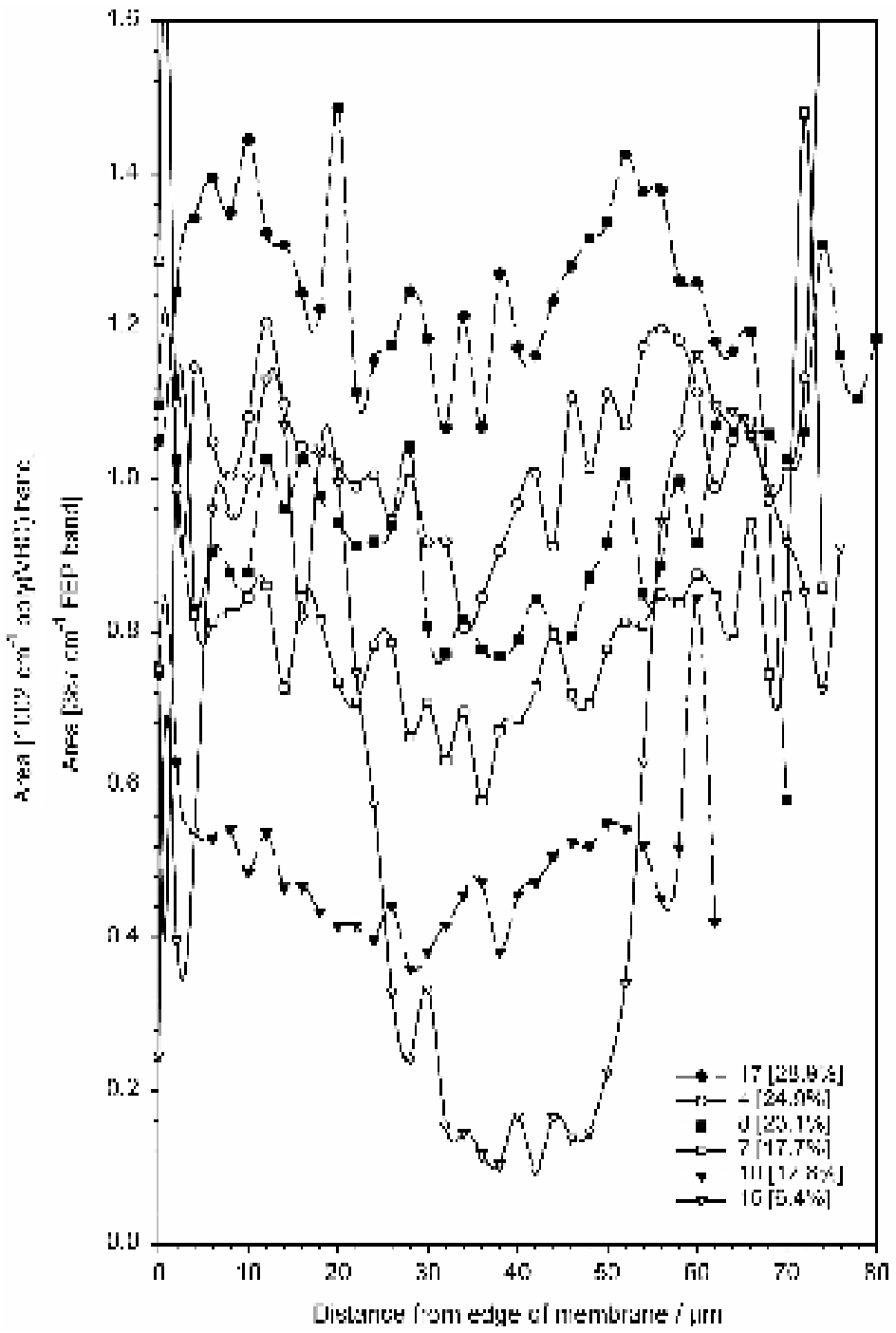
1.6
1.4
1.2
1.0
0.8
0.6
0.4
0.2
0.0
0
10
20
30
40
50
60
70
80
Distance from edge of membrane / μm
17 [25.9%]
- [24.0%]
0 [23.1%]
7 [17.7%]
10 [17.8%]
16 [5.4%]

Figure 8

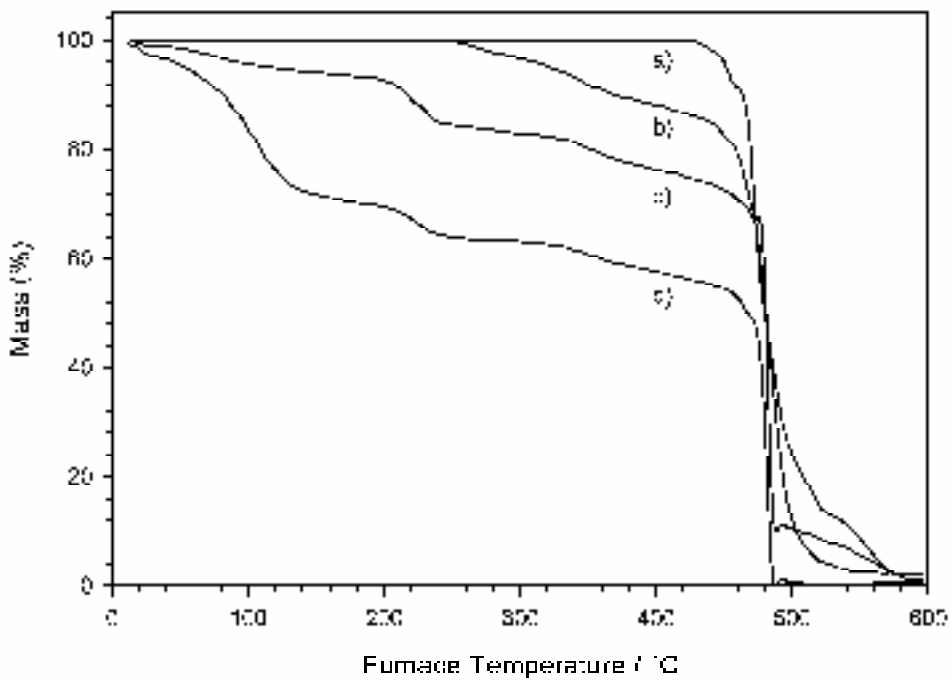
100
80
60
40
20
0
Mass (%)
a)
b)
c)
d)
0
100
200
300
400
500
600
Furnace Temperature / °C

Figure 9

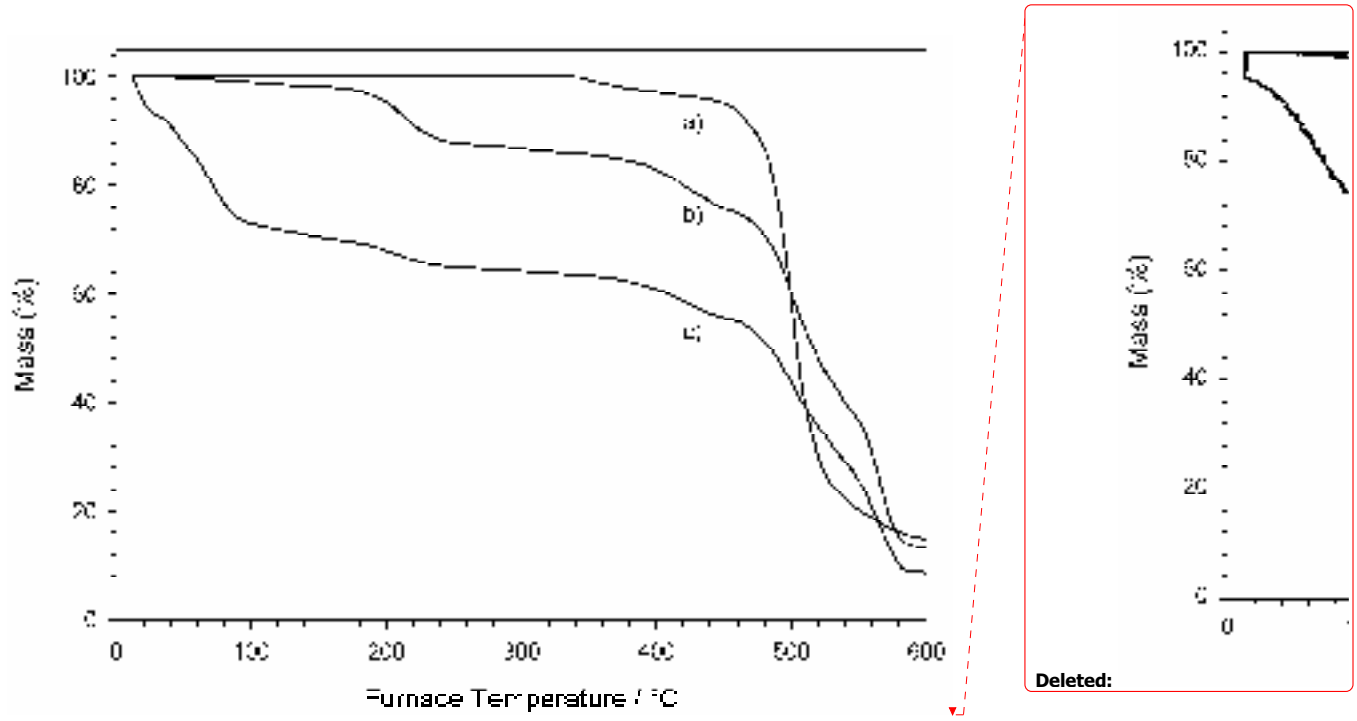
Mass (%)
Furnace Temperature / °C
a)
b)
c)
0
100
200
300
400
500
600
Deleted:

Figure 10